EFFECTS OF BISMARCK BROWN DYE ON THE CRYSTALLIZATION KINETICS OF POTASSIUM ALUM IN A CMSMPR CRYSTALLIZER

CLIFFORD Y. TAI, JENN-FANG WU AND LII-PING LEU
Department of Chemical Engineering, National Taiwan University, Taipei, Taiwan 10764

Key Words:

This study examined the effects of an additive, Bismarck Brown dye, on the crystallization kinetics of potassium alum crystals in a well-mixed continuous crystallizer. In the data analysis, size-dependent growth kinetics was assumed. The addition of Bismarck Brown dye depressed crystal growth and nucleation rates. The supersaturation of solution at steady state in the crystallizer increased as the Bismarck Brown concentration increased under the constraint of constant retention time and magma density. In this case the growth rate was enhanced but the nucleation rate was reduced. The predicted kinetic behaviors influenced by the addition of Bismarck Brown dye were in good agreement with the experimental results.

Introduction

The crystal size distribution in a continuous mixed-suspension mixed-product removal (CMSMPR) crystallizer is generally influenced by several factors, including supersaturation level, suspension density, agitation speed, system temperature, and impurity concentration. The effects of these factors on the crystallization kinetics, *i.e.*, crystal growth and nucleation rates, have been reviewed by Garside and Shah[2], Garside[1], and Tavare[17]. Among the factors, the effect of additive as impurity is less understood because the problem itself is more complicated, and relatively little work has been done in this area.

Regarding the impurity effect, most of the crystal growth rate and nucleation rate data are compared under the constraint of constant magma density. A survey of experimental studies of impurity effects is presented in **Table 1**. The systems studied are inorganic crystals, and the additives as impurity include ionic species, organic compounds, surface-active agents, and dyestuff. No general conclusions can be drawn from the table. It should be noted that the crystal growth rate and nucleation rate are compared at constant magma density and the supersaturation of solution was not measured in the experiments of the early works shown in Table 1; an increase in crystal growth rate is accompanied by a decrease in nucleation

Table 1. Survey of impurity effects on crystal growth and nucleation rates in a CMSMPR Crystallizer

System	Impurity	Response to increasing impurity conc.	Operation mode	Techniques of measuring σ	Reference
KNO_3	Co^{2+}, Cr^{3+}	$B°\downarrow$ $G°\uparrow$	steady-state	*	(12)
KNO_3	$CH_3NH_2 \cdot HCl$, $CH_3(NH_2)_{11}NH_2 \cdot HCl$, FC-98	$B°\uparrow$ $G°\downarrow$	steady-state	*	(12)
NaCl	Pb^{2+}	$B°\downarrow$ $G°\uparrow$	steady-state	*	(5)
$(NH_4)_2SO_4$	Cr^{3+}	$B°\downarrow$ $G°\uparrow$	steady-state	*	(4)
Potassium Alum	Quinoline Yellow dye	$B°?$ $G°\downarrow$	steady-state	*	(11)
Borax	Conoco 500, Sodium oleate, Sodium lauryl sulfate	$B°\downarrow$ $G°\downarrow$	quasi steady-state	refractometer	(8)
Borax	NaCl, $MgCl_2$	$B°\uparrow$ $G°\downarrow$	quasi steady-state	refractometer	(8)
Ammonium Alum	Cr^{3+}, Fe^{3+}, Na^+	$B°\uparrow$ $G°\uparrow$	steady-state	refractometer	(18)
Potassium Alum	Bismarck Brown dye	$B°\downarrow$ $G°\downarrow$	steady-state	density meter	this study

* Supersaturation was not reported.

* Received May 6, 1992. Correspondence concerning this article should be addressed to C. Y. Tai.

rate or vice versa. Tai[13] has explained how this could possibly happen when the supersaturation at steady state shifts to a different level by adding impurities to a CMSMPR crystallizer. In the report the analysis was illustrated by a size-independent system.

In this study, we considered size-dependent growth of potassium alum crystals in experiments with the CMSMPR crystallizer and developed a detailed analysis of impurity effects on crystal growth and nucleation rates, using power-law models to represent the two rate equations. The concentration of potassium alum in the solution was determined by a density meter. The crystal growth and nucleation rates were obtained from the crystal size distribution at steady state. Under the constraint of constant magma density and retention time, the predicted behaviors of crystallization kinetics influenced by the addition of impurity were compared with the experimental results.

1. Population Balance and Crystallization Kinetics

When a CMSMPR crystallizer is operated at steady state with no crystal breakage and no crystals in the feed stream, the number balance on the crystals in the crystallizer leads to the following equation:

$$\frac{d(Gn)}{dL} = -\frac{n}{\tau} \tag{1}$$

Assuming that the crystal growth rate follows the ASL model[11],

$$G = G^\circ(1+\gamma L)^b ; \qquad b<1 \tag{2}$$

The parameter γ in Eq. (2) is often set equal to $1/G^\circ\tau$ in order to reduce the number of parameters and thus to simplify the calculation. Substituting Eq. (2) into Eq. (1), we may solve the resulting differential equation to give the crystal size distribution,

$$n = n^\circ\left(1+\frac{L}{G^\circ\tau}\right)^{-b}\exp\left[\frac{1-(1+L/G^\circ\tau)^{1-b}}{1-b}\right] \tag{3}$$

The suspension density M_t is integrated to give[6]:

$$M_t = K_v\rho\int_0^\infty L^3 n dL = C_1(b)K_v\rho n^\circ(G^\circ\tau)^4 \tag{4}$$

The function $C_1(b)$ is expressed by Rousseau and Parks[10] as:

$$C_1(b) = \exp[1.79+4.27b-14.97b^2+71.96b^3 -121.25b^4+79.05b^5] \tag{5}$$

Substituting Eq. (4) into Eq. (3) to eliminate n°,

$$n = \frac{M_t}{C_1(b)K_v\rho(G^\circ\tau)^4}\left[1+\frac{L}{G^\circ\tau}\right]^{-b} \cdot\exp\left[\frac{1-(1+L/G^\circ\tau)^{1-b}}{1-b}\right] \tag{6}$$

Eq. (6) is used for estimating G° and b by fitting the experimental data of population density.

The nucleation rate of nuclei is related to the nuclei growth rate and nuclei population density.

$$B^\circ = G^\circ n^\circ \tag{7}$$

Because secondary nucleation is the dominating mechanism in a stirred crystallizer, the growth and nucleation rates are frequently related to the state variables by the power-law kinetic models,

$$G^\circ = K_g\sigma^{n_g}C_i^{k_g} \tag{8}$$

and

$$B^\circ = K_b\sigma^{n_b}C_i^{n_b}M_t^j \tag{9}$$

Substitution of Eqs. (7)–(9) into Eq. (4) gives an expression of supersaturation,

$$\sigma = \left(\frac{C_i^{-(k_n+3k_g)}}{C_1(b)K_v\rho K_b K_g^3\tau^4 M_t^{i-1}}\right)^{1/n_g(i+3)} \tag{10}$$

where $i=n_b/n_g$. Supposing that the supersaturation is too small to measure, Eq. (10) can be substituted into Eqs. (8) and (9) to give expressions of crystal growth and nucleation rates without knowing the supersaturation:

$$G^\circ = \left(\frac{K_g^i}{C_1(b)K_v\rho K_b}\right)^{1/(i+3)} M_t^{(1-j)/(i+3)}\tau^{-4/(i+3)} \cdot C_i^{-(k_n-ik_g)/(i+3)} \tag{11}$$

and

$$B^\circ = \left(\frac{K_b^{3/i}}{C_1(b)K_v\rho K_b}\right)^{i/(i+3)} M_t^{(i+3j)/(i+3)}\tau^{-4i/(i+3)} \cdot C_i^{3(k_n-ik_g)/(i+3)} \tag{12}$$

From Eqs. (11) and (12) it can be seen that the influence of impurity on the crystal growth rate and nucleation rate would be in an opposite direction under the constraint of constant production rate, *i.e.*, constant magma density and retention time. The slope of the plot of B° versus C_i and the slope of G° versus C_i on a logarithmic scale would differ by a factor of -3. The effect of increasing impurity concentration on the supersaturation, growth rate and nucleation rate will depend on the values of k_g, k_n, and i. The analysis is similar to the size-independent system that has been discussed by Tai[13], and is summarized in **Table 2**. In the table, the values of k_g and i are assumed to be negative and positive respectively. That happens to be the case in this study.

2. Experimental Procedure

This experimental section is essentially the same as that reported by Wu *et al.*[19] in a previous paper reporting the effects of temperature on the crystallization kinetics of the same crystal, except that an

Table 2. Effect of increasing impurity concentration on nucleation and growth rates as a function of k_n/k_g for constant τ and constant M_t in a CMSMPR crystallizer

k_n/k_g*		$k_n - ik_g$	Supersaturation σ	Growth rate G°	Nucleation rate B°
$k_n/k_g < -3$	$(k_n + 3k_g > 0)$	>0	↓	↓	↑
$k_n/k_g = -3$	$(k_n + 3k_a = 0)$	>0	—	↓	↑
	$-3 < k_n/k_g < 0$	>0	↑	↓	↑
	$k_n/k_g = 0$ $(k_n = 0)$	>0	↑	↓	↑
$k_n/k_g > -3$ $(k_n + 3k_g < 0)$	$0 < k_n/k_g < i$**	>0	↑	↓	↑
	$k_n/k_g = i$	$=0$	↑	—	—
	$k_n/k_g > i$	<0	↑	↑	↓

* k_g is assumed to be negative.
** i is assumed to be positive.

impurity (Bismarck Brown) was added to the potassium alum solution. It is worth mention that a measurable supersaturation was sustained in the solution at steady-state operation, and was determined by use of a density meter. The procedures were as follows. At steady state a slurry sample was withdrawn from the crystallizer and quickly filtered by use of a vacuum system to separate the slurry into cake and filtrate. The cake was subjected to size annalysis after drying and the density of the filtrate was measured by a density meter (Kyoto Electronics, DA-210). Then the density of the solution was converted to concentration *via* a pre-calibrated density-concentration curve. Once the concentration of solution is available, the relative supersaturation of the system at steady state is calculated as

$$\sigma = (c - c^*)/c^* \tag{13}$$

In this experiment Bismarck Brown dye was chosen as impurity because dyestuffs have long been used as crystal habit modifiers in the industry. However, the crystal habit of potassium alum was not altered by the addition of Bismark Brown into the solution up to a concentration of 500 ppm. The dye has this molecular structure:

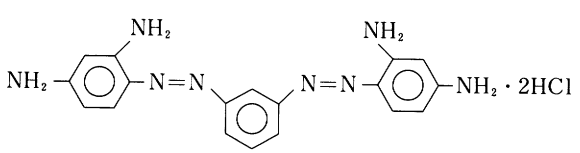

(14)

When it dissolves in water, a large cation forms to give the brown color.

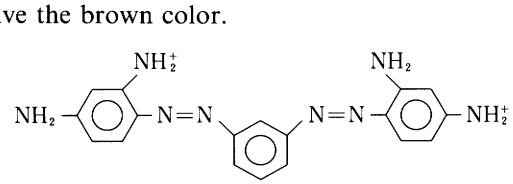

(15)

The concentration of Bismarck Brown dye was determined by an UV spectrophotometer; the concentration range investigated in this study was 5 to 500 ppm. It should be noted that the addition of Bismarck Brown dye does change the solubility of potassium alum when the dye concentration is higher than 50 ppm. For example, the solubility increases by 0.30 kg hydrate/100 kg H_2O at 500 ppm dye concentration. This effect has been taken into account.

The crystal mass distribution of a sample was determined by a sieve for crystal size $(251\text{–}1245) \times 10^{-6}$ m, and by a Microtrac particle size analyzer for crystal size $(2\text{–}251) \times 10^{-6}$ m. Then the population densities were calculated from crystal mass distributions[9].

3. Results

Sixteen runs were performed at 293 K in this study, in which potassium alum was crystallized out from an aqueous solution with Bismarck Brown added as impurity. Population densities were determined from crystal mass distribution data. From population density data a nonlinear least-square parameter estimation program, a random search method, was used to search for b and G° in Eq. (6)[19]. A typical population density curve is presented in **Fig. 1**, which looks similar to those presented by Rousseau and Woo[11] and Wu *et al.*[19], *i.e.*, curvature over the entire size range, indicating that the crystal growth rate is possibly size-dependent. Once G° is available, n° can be evaluated by Eq. (4). Then we obtain B° from Eq. (7). The values of B° and G° of each run are collected in **Table 3**, along with other model parameters and system variables.

Assuming that the suspension density, relative supersaturation, and impurity concentration are independent variables, we obtained the nuclei growth rate and nucleation rate equations by use of a regression analysis.

$$G^\circ = 1.227 \times 10^{-6} \sigma^{1.632} C_i^{-0.0465} \tag{16}$$

and

$$B^\circ = 2.987 \times 10^{10} \sigma^{3.225} M_t^{1.026} C_i^{-0.2416} \tag{17}$$

Table 3. Values of system variables and model parameters for various residence times and different Bismarck Brown dye concentrations, $T=293$ K

Run no.	C_i	σ	$G^\circ \times 10^8$	$B^\circ \times 10^{-7}$	M_t (from solute balance)	M_t (exp.)	τ	b
1	5	0.07581	1.257	12.35	24.71	27.19	1240	0.479
2	5	0.10119	2.007	31.26	19.99	21.34	640	0.492
3	5	0.05392	1.350	3.542	26.50	26.54	1800	0.406
4	5	0.04167	0.938	2.956	27.81	27.20	2360	0.441
5	10	0.06968	0.995	14.47	23.99	23.41	1240	0.531
6	20	0.07133	1.921	5.268	22.71	23.69	1240	0.391
7	50	0.07377	1.501	7.175	21.61	21.89	1240	0.448
8	50	0.08515	4.108	8.662	19.66	20.18	670	0.303
9	50	0.06677	0.817	3.280	21.99	23.17	2310	0.476
10	100	0.08574	1.579	5.799	19.56	20.17	1240	0.445
11	200	0.08779	1.762	4.368	19.38	19.85	1240	0.435
12	200	0.08779	2.532	22.80	19.74	19.37	620	0.437
13	200	0.06768	0.941	1.973	21.71	22.98	2390	0.467
14	500	0.08696	1.258	7.025	18.46	18.56	1240	0.504
15	500	0.08085	1.004	1.922	20.30	21.64	2360	0.441
16	500	0.09132	3.665	11.02	17.44	16.21	630	0.326

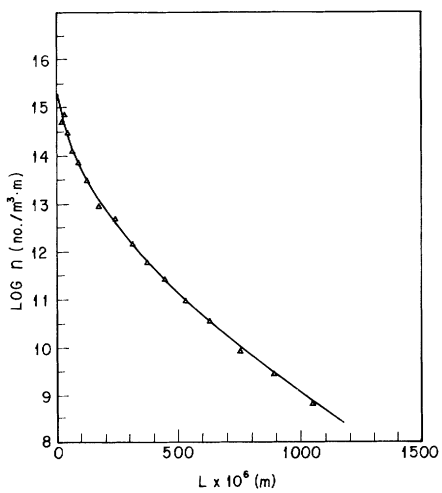

Fig. 1. Population density plot of Run 13C
— Eq. (6), $G^\circ = 9.405 \times 10^{-9}$ m/s
$b = 0.4672$
△ Experimental data

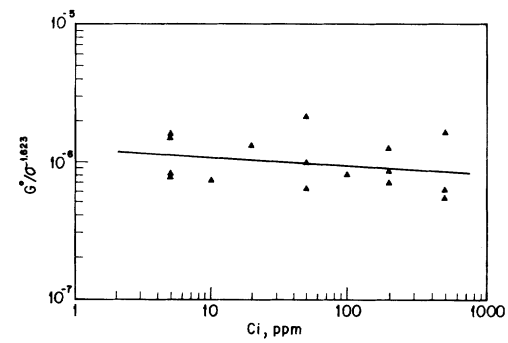

Fig. 2. Effect of Bismarck Brown dye on the crystal growth rate of potassium alum

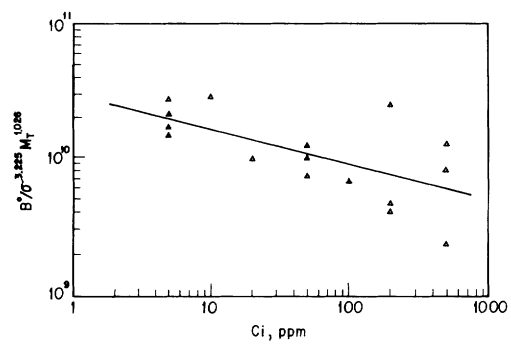

Fig. 3. Effect of Bismarck Brown dye on the nucleation rate of potassium alum

Because M_t does not change much in the impure runs shown in Table 3, it is impossible to obtain j from growth rate data of the impure system by regression method. Therefore, j was set at 1.026 of the pure-system value.

The presence of Bismarck Brown dye has an influence on the crystal growth rate and nucleation rate as shown in **Figs. 2** and **3** respectively; both kinetic rates were depressed.

4. Discussion

The values of b determined in this study varied between 0.30 and 0.53, but were nearly independent of impurity concentration. The values are slightly lower than the values, 0.42–0.57, found in the previous experiment with the system operated at the same temperature[19]. The variation of b has been observed in several studies and is attributed to the dependence of b on the process conditions[3,10,19].

In searching for the parameters in the nucleation rate equation, j was set to 1 in most of the MSMPR studies listed by Garside and Shah[2]. In this study the exponent of M_t was found to be 1.026, which is very close to 1, by a linear regression analysis, using the growth rate data of pure system. Otten and de Jong[7]

inferred that the crystal-wall and crystal-impeller collision should be the major mechanisms of nucleation for this type of kinetics.

The supersaturation sustained in an MSMPR crystallizer is usually low for many systems, which are classified as Class II systems by Randolph and Larson[9]. To avoid the measurement of supersaturation, the nucleation rate was often correlated with the crystal growth rate in the literature. Such a correlation can be obtained by combining Eqs. (8) and (9),

$$B^\circ = \frac{K_b}{K_g^i}(G^\circ)^i M_t^j C_i^{k_n - ik_g} \tag{18}$$

The parameters in Eq. (18) could be found in Eqs. (16) and (17), and the correlation is:

$$B^\circ = 1.664 \times 10^{22}(G^\circ)^{1.987} M_t^{1.026} C_i^{-0.149} \tag{19}$$

To illustrate the impurity effect on the nucleation and crystal growth rates under the constraint of constant magma density and retention time, *i.e.*, constant production rate, we define G^* and B^* as the following forms because it is extremely difficult to keep M_t and τ constant from run to run.

$$G^* = G^\circ[C_1(b)]^{1/(i+3)}/(M_t^{(1-j)/(i+3)})(\tau^{-4/(i+3)}) \tag{20}$$

and

$$B^* = B^\circ[C_1(b)]^{i/(i+3)}/(M_t^{(i+3j)/(i+3)})(\tau^{-4i/(i+3)}) \tag{21}$$

When Eqs. (11) and (12) are substituted into Eqs. (20) and (21) respectively, and then the values of constants and parameters are substituted into the resultant equations, we have:

$$G^* = K_g^{i/(i+3)} K_b^{-1/(i+3)}(\rho K_v)^{-1/(i+3)} C_i^{(ik_g - k_n)/(i+3)}$$
$$= 8.909 \times 10^{-6} C_i^{0.030} \tag{22}$$

and

$$B^* = K_g^{-3i/(i+3)} K_b^{-3/(i+3)}(\rho K_v)^{-i/(i+3)} C_i^{-3(ik_g - k_n)/(i+3)}$$
$$= 1.54 \times 10^{12} C_i^{-0.090} \tag{23}$$

Eqs. (22) and (23) are plotted in **Figs. 4** and **5**, respectively. Data points, calculated by Eqs. (20) and (21) using experimentally determined values of i, j, G°, B°, $C_1(b)$, M_t, and τ, are also shown in the figures. Although data points were scattered in a range shown in the figures, the arithmetic mean at each impurity concentration level was fairly close to that predicted by Eqs. (22) and (23).

In the early studies of the impurity effect shown in Table 1, the supersaturation of the system was not measured and an increase in nucleation rate is accompanied by a decrease in growth rate or vice versa. This is consistent with the prediction of Eqs. (11) and (12), when the MSPMR crystallizer is operated under the constraint of constant magma

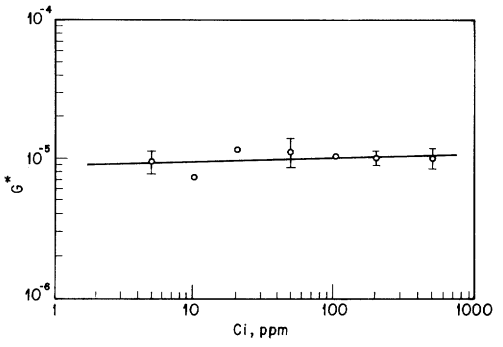

Fig. 4. Impurity effect on the crystal growth rate under the constraint of constant production rate
◦ data points
— Eq. (22)

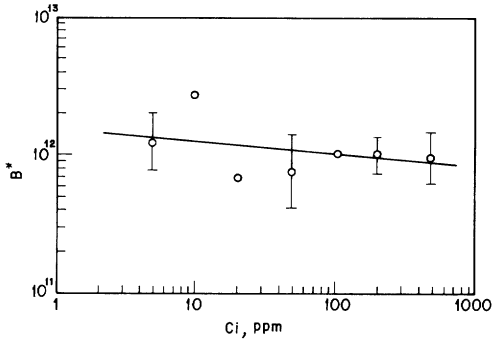

Fig. 5. Impurity effect on the nucleation rate under the constraint of constant production rate
◦ data points
— Eq. (22)

density and retention time. It means that the observed kinetic behavior is a combined result of impurity and supersaturation effects. In this study, the value of $(k_n + 3k_g)$ is negative so that the supersaturation would be higher at higher impurity concentration as indicated by Eq. (10).

The diffusion step to transport solute from bulk solution to the solid-liquid interface has no effect on the crystal growth rate when the dye concentration is low[14]. Therefore, the decrease in growth rate of potassium alum in this study was attributed to a reduction in the surface integration rate. A blocking effect has been widely accepted for the reduction of surface integration rate, *i.e.*, dye molecules being adsorbed onto some of the available sites for growth on the crystal surface so that the integration rate of growth units is reduced. Besides, the order of supersaturation in the growth rate equation was altered, changing from 2.0 for pure system[19] to 1.632 for impure system. This kinetic behavior has been observed by Tai *et al.*[16]. In their report, the surface integration order of magnesium sulfate changed gradually from first to second when a small amount of chromium chloride was added to the system. They offered a possible mechanism for such a change, using

the BCF theory.

How the adsorbed dye molecules affect the nucleation rate is less understood. It may be due to a change in solubility on the crystal surface, or a reduction in the number of nuclei in the nuclei-generation stage, or a decrease in the fraction of nuclei surviving in the nuclei-growth stage[15]. Among these the reduction in the number in the generation stage is the most likely mechanism, since the nuclei were induced by secondary nucleation in a continuous crystallizer and the nuclei-generation stage is most sensitive to a change in crystal-growing environment. To explore a possible mechanism of impurity effect a hypothesis related to the source of secondary nuclei, suggested by Tai *et al.*,[15] should be described. A semi-ordered, partially desolvated layer of solute *i.e.*, adsorption layer, exists at the solution-solid interface. The clusters queue up in the layer awaiting incorporation into the growing crystal. After they migrate into the adsorption layer, the chemical bonds between them partially break to release some of the solvated water, and the clusters reform to become larger in size along their path to the crystal surface. Then, they finally reach the crystal surface to become a growth unit which is ready to integrate into the crystal lattice. When a force is applied to the crystal surface, either by contact or shear force, the clusters are swept off to the bulk of solution. Then the clusters, with a size distribution, will grow to become crystals or dissolve to lose their identity, depending on the supersaturation of bulk solution. Since the integration rate of growth units has been reduced by the absorption of dye molecules, the structure of the adsorption layer is possibly affected. The role played by the dye molecules is not exactly known, but they may reduce the desolvation rate of clusters or decrease the average size of clusters in the adsorption layer. As a result, the number of clusters available for nucleation decreases in either case, thus reducing the nucleation rate.

5. Conclusion

When impurity is added to an MSMPR crystallizer, the observed kinetics could result from the combined effects of impurity and supersaturation. To see the impurity effect alone, the supersaturation in the crystallizer should be measured with care since it is usually low under steady-state operation. A density meter was successfully applied to determine the supersaturation of the system in this study.

The crystal growth rate of potassium alum appeared to be size-dependent. The presence of Bismarck Brown dye in the solution depressed the growth and nucleation rates of the crystal. Under the constraint of constant magma density and retention time, the addition of dye would increase the supersaturation level and crystal growth rate, but decrease the nucleation rate.

The mechanism of impurity effect on the crystallization kinetics might be complex, but the effect of dyestuff is rather simple; the adsorbed dye molecules on the crystal-solution interface block the available sites for growth and reduce the number of clusters available for nucleation. The concentration of Bismarck Brown dye can be incorporated into the power-law kinetic expressions to describe the kinetic behaviors, which were in agreement with experimental data. Besides, the reaction order with respect to supersaturation in the crystal growth rate was altered by the addition of Bismarck Brown dye. BCF theory can be used to explain this type of crystal growth kinetics.

Acknowledgement

The authors gratefully acknowledge the support of the National Science Council of the Republic of China through Grant NSC 77-0402-E002-09.

Nomenclature

B°	=	nucleation rate	[no./m^3·s]
B^*	=	nucleation rate function defined in Eq. (22)	[no./m^3·s]
b	=	kinetic parameter in ASL growth rate equation	[—]
C	=	solution concentration in crystallizer	[kg hydrate/kg free water]
C_i	=	impurity concentration	[ppm]
C^*	=	solution concentration at saturation	[kg hydrate/kg free water]
$C_1(b)$	=	moment coefficient defined in Eq. (5) for the two-parameter ASL model	[—]
G	=	crystal growth rate	[m/s]
G°	=	nuclei growth rate	[m/s]
G^*	=	growth rate function defined in Eq. (20)	[m/s]
i	=	relative kinetic order, n_b/n_g	[—]
j	=	kinetic order of suspension density in nucleation rate equation	[—]
K_b	=	nucleation rate constant; its units depend on n_b, k_n and j.	
K_g	=	growth rate constant; its units depeend on n_g and k_g	
K_v	=	volumetric shape factor	[—]
k_g	=	kinetic order of supersaturation in nucleation rate model	[—]
k_n	=	kinetic order of supersaturation in growth rate model	[—]
L	=	equivalent diameter of crystal size	[m]
M_t	=	magma density	[kg/m^3]
n	=	population density	[no./m^3·m]
n°	=	population density of nuclei	[no./m^3·m]
γ	=	parameters in the ASL growth rate equation	[—]
ρ	=	crystal density	[kg/m^3]
τ	=	retention time	[s]
σ	=	relative supersaturation, $(C-C^*)/C^*$	[—]

Literature Cited

1) Garside J.: *Chem. Eng. Sci.*, **40**, 3 (1985).
2) Garside J. and M. B. Shah: Ind. Eng. Chem. Process Des. Dev., 19,509 (1980).
3) Garside, J. and S. J. Jancic: *Chem. Eng. Sci.*, **33**, 1623 (1978).
4) Larson, M. A. and J. W. Mullin: *J. Crystal Growth*, **20**, 183 (1973).
5) Liu, Y. A. and G. D. Botsaris: *AIChE J.*, **19**, 510 (1973).
6) O'Dell, F. P. and R. W. Rousseau: *AIChE J.*, **24**, 738 (1978).
7) Otten, E. P. K. and E. J. de Jong: *Ind. Eng. Chem. Fundam.*, **12**, 179 (1973).
8) Randolph, A. D. and A. D. Puri: *AIChE J.*, **27**, 92 (1981).
9) Randolph, A. D. and M. A. Larson, "Theory of Particulate Processes", Academic Press, Inc., San Diego, California (1988).
10) Rousseau, R. W. and R. M. Parks: *Ind. Eng. Chem. Fundam.*, **20**, 71 (1981).
11) Rousseau, R. W. and R. Woo: *AIChE Symp. Ser.*, **76** (NO. 193), 27 (1980).
12) Shor, S. M. and M. A. Larson: *CEP Symp. Ser.*, **67** (NO. 110), 32 (1971).
13) Tai, C. Y.: *J. Chin. I.Ch.E.*, **16**, 179 (1985).
14) Tai, C. Y., C. Y. Chen, and J. F. Eu: *Chem. Eng. Commun.*, **56**, 329 (1987).
15) Tai, C. Y., J.-F. Wu, and R. W. Rousseau: *J. Crystal Growth*, **116**, 294 (1992).
16) Tai, C. Y., C.-S. Cheng, and Y.-C. Huang, Accepted for publication, in J. Cryst. Growth (1992).
17) Tavare, N. S.: *AIChE J.*, **32**, 705 (1986).
18) Teodossiev, N. and E. Kirkova, Ind. Cryst. 84, ed. S. J. Jancic and E. J. de Jong, pp. 305–308, Elsevier Science Publishers, Amsterdam (1984).
19) Wu, J. F., C. Y. Tai, W. K. Yang, and L. P. Leu: *I&EC Research*, **30**, 2226 (1991).